

LETTER TO THE EDITOR

The longest period transiting planet candidate from *K2*

H.A.C. Giles^{1,*}, H.P. Osborn², S. Blanco-Cuaresma³, C. Lovis¹, D. Bayliss⁴, P. Eggenberger¹,
A. Collier Cameron⁵, M.H. Kristiansen^{6,7}, O. Turner¹, F. Bouchy¹, and S. Udry¹

¹ Observatoire de Genève, Université de Genève, Chemin des Maillettes 51, 1290 Versoix, Switzerland
e-mail: Helen.Giles@unige.ch

² Aix Marseille Univ, CNRS, LAM, Laboratoire d'Astrophysique de Marseille, Marseille, France

³ Harvard-Smithsonian Center for Astrophysics, 60 Garden Street, Cambridge, MA 02138, USA

⁴ Department of Physics, University of Warwick, Gibbet Hill Road, Coventry, CV4 7AL, UK

⁵ Centre for Exoplanet Science, SUPA, School of Physics and Astronomy, University of St Andrews, North Haugh, St Andrews KY16 9SS, UK

⁶ DTU Space, National Space Institute, Technical University of Denmark, Elektrovej 327, DK-2800 Lyngby, Denmark

⁷ Brorfelde Observatory, Observator Gyldenkerens Vej 7, DK-4340 Tølløse, Denmark

Received June **Date**, 2018; accepted June **Date**, 2018

ABSTRACT

Context. We present the transit and follow-up of a single transit event from Campaign 14 of *K2*, EPIC248847494b, which has a duration of 54 hours and a 0.18%-depth.

Aims. Using photometric tools and conducting radial velocity follow-up, we vet and characterise this very strong candidate.

Methods. Due to a long, unknown period, standard follow-up methods need to be adapted. The transit is fitted using *Namaste*, and the radial velocity slope measured and compared to a grid of planet-like orbits with varying masses and periods. These utilised stellar parameters measured from spectra and the distance as measured by *Gaia*.

Results. Orbiting around a sub-giant star with a radius of $2.70 \pm 0.12 R_{\text{Sol}}$, the planet has a radius of $1.11^{+0.07}_{-0.07} R_{\text{Jup}}$ and a period of 3650^{+1280}_{-1130} days. The radial velocity measurements constrain the mass to be less than $13 M_{\text{Jup}}$, which implies a planetary-like object.

Conclusions. We have found a planet at 4.5 AU from a single transit event. After a full radial velocity follow-up campaign, if confirmed, it will be the longest-period transiting planet discovered.

Key words. Planets and satellites: detection – Stars: individual:EPIC248847494 – EPIC248847494: planetary systems – Techniques: photometric, Techniques: radial velocities – Techniques: spectroscopic

1. Introduction

Detecting exoplanets via single transit events (monotransits) will be crucial in the era of short duration (27 day) *TESS* campaigns, with over 1000 monotransits estimated (Villanueva et al. 2018). To date, a number of monotransit candidates have been proposed (Osborn et al. 2016; LaCourse & Jacobs 2018; Osborn et al. in prep.; Vanderburg et al. 2018). Of the 160+ candidates in LaCourse & Jacobs (2018), they also report the detection of the monotransit reported in this work. However, currently only one has been confirmed and re-observed (HIP116454b, Vanderburg et al. 2015), on a 9.1-day orbit.

We report the discovery of EPIC248847494b, a sub-stellar object on a very long-period orbit which exhibited a single transit in Campaign 14 of *K2*. In Section 2, we outline the observations taken leading to and following the detection. In Section 3, we describe the analysis of the data to characterise the system, and the processes taken to eliminating other causes. In Section 4, we discuss the implications of this planet-like object; and in Section 5, we summarize the discovery.

2. Observations

EPIC248847494b was observed in Campaign 14 of the *K2* mission in long cadence (29.4 minute exposures). The campaign began on 1st June 2017 at 05:06:29 UTC and ended 19th August 2017 at 22:11:02 UTC, lasting 79.7 days.

Following the public release of *K2* reduced data on 20th November 2017, the light curves were searched for planetary signals following the same method as described in Giles et al. (2018). This utilised the *K2* PDC_SAP-reduced light curves which were detrended using a moving polynomial and removing significant outliers; then searching for transits using a box-fitting least squares algorithm (BLS, Kovács et al. 2002). In addition to regular transit candidates, we detected a single transit event in the light curve of EPIC248847494 (see Fig. 1). The transit depth is approximately 1.7 mmag, lasting over 53 hours. No other transits or unusual systematics were seen in the light curve. From this we concluded that the event was of astrophysical origin.

In order to determine the nature of this very strong candidate, we observed EPIC248847494 with the 1.2m Euler telescope at La Silla Observatory in Chile using the CORALIE spectrograph (Queloz et al. 2000). CORALIE is a fibre-fed, high resolution ($R=60,000$) echelle spectrograph which is capable of high precision ($< 6 \text{ m s}^{-1}$) radial velocity measurements (RVs). 15 observations were taken between 17th December 2017 and 17th April 2018 (see Table 1) where a 16th point was removed due to sig-

* Email: Helen.Giles@unige.ch

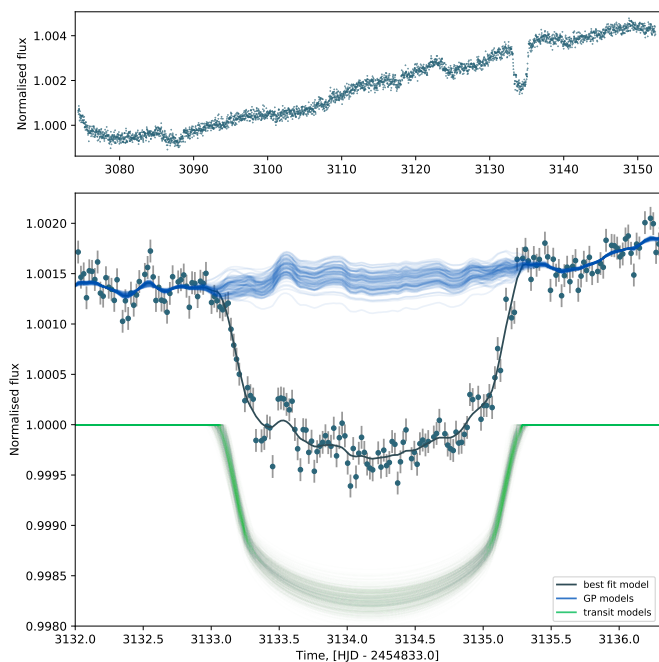


Fig. 1. Transit of EPIC248847494b observed by *K2* and Namaste models. Upper panel shows the full light curve while the lower panel shows a zoom of the transit, and the models. The black line shows the best-fit Namaste model. This is composed of the transit model (100 randomly selected models shown in green), and Gaussian Process realisations (blue).

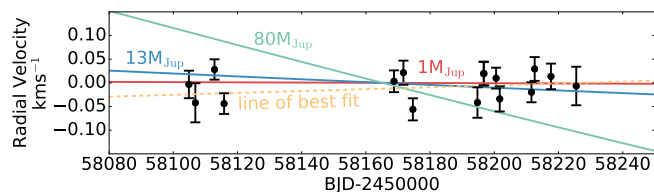


Fig. 2. Radial velocity observations from CORALIE (black points) compared with circular-orbit models of three objects: a Jupiter-mass planet (red), a $13M_{\text{Jup}}$ brown dwarf (blue) and a $80M_{\text{Jup}}$ low-mass star (green) assuming a period of 3650 days. The yellow dashed line is the line of best fit (see Sect. 2).

nificantly high instrumental drift. These points give an RV slope of $0.19 \pm 0.16 \text{ m s}^{-1} \text{ day}^{-1}$ (Fig. 2).

To check that radial velocity variations were not due to a blended spectrum, we compute the bisector slope of the cross-correlation function for each observation as described by Queloz et al. (2001), see Table 1. We see no correlation between the bisector slope and radial velocities. We also recompute using different stellar masks and see no trends which suggests this is not a blended binary (Bouchy et al. 2009).

3. Analysis

3.1. Stellar Parameters

To determine the stellar parameters of EPIC248847494, we followed the same methodology as Giles et al. (2018). A pipeline was built for the CORALIE spectra based on *iSpec*¹ (Blanco-Cuaresma et al. 2014a). All observations were aligned and

¹ <http://www.blancocuaresma.com/s/iSpec>

Table 1. CORALIE Radial Velocities of EPIC248847494

BJD-2450000	RV [kms^{-1}]	RV Error [kms^{-1}]	BIS
8104.845468	29.088	0.029	0.015
8106.856642	29.050	0.041	0.001
8112.830676	29.120	0.022	-0.061
8115.818047	29.048	0.022	-0.020
8168.748372	29.095	0.023	0.000
8171.685229	29.113	0.025	-0.061
8174.628598	29.036	0.023	-0.036
8194.743602	29.050	0.032	-0.034
8196.710862	29.111	0.025	-0.010
8200.554695	29.102	0.022	-0.004
8201.685863	29.058	0.027	-0.001
8211.576046	29.072	0.021	-0.011
8212.572145	29.121	0.025	-0.055
8217.646377	29.105	0.027	-0.037
8225.522768	29.085	0.041	-0.038

co-added to increase S/N, reduced and spectrally fitted using: SPECTRUM (Gray & Corbally 1994) as the radiative transfer code; atomic data obtained from the Gaia-ESO Survey line list (Heiter et al. 2015b); line selection based on a $R \sim 47\,000$ solar spectrum (Blanco-Cuaresma et al. 2016, 2017); and the MARCS model atmospheres (Gustafsson et al. 2008). Resulting errors were increased by quadratically adding the dispersions found when analyzing the Gaia benchmark stars (Heiter et al. 2015a; Jofré et al. 2014; Blanco-Cuaresma et al. 2014b) with the same pipeline. This resulted in an effective temperature of $4877 \pm 68 \text{ K}$, a $\log g$ of $3.41 \pm 0.07 \text{ dex}$ and $[\text{Fe}/\text{H}] = -0.24 \pm 0.04 \text{ dex}$.

From the second data release of Gaia (Gaia Collaboration et al. 2018), EPIC248847494 has a measured parallax (see Table 2) from which we can determine an independent stellar radius using bolometric absolute magnitudes and the spectroscopically determined effective temperature for EPIC248847494 following the method detailed in Fulton & Petigura (2018). We take the K-band apparent magnitude (Skrutskie et al. 2006), the Gaia distance and a bolometric correction (BC_K , from Houdashelt et al. 2000) of 1.91 ± 0.05 which was interpolated from the range within the coarse grid. We chose not to include an extinction correction as this only introduces an uncertainty of 0.5% (Fulton & Petigura 2018). This gave a radius of $2.70 \pm 0.12 R_{\text{sol}}$.

Taking the spectrally-determined metallicity and effective temperature, and the measured radius as observational constraints, we input them into the Geneva stellar evolution code (Eggenberger et al. 2008). This results in a stellar mass of $0.9 \pm 0.09 M_{\text{sol}}$. These values of mass and radius would therefore indicate a $\log g$ of 3.52 dex. If we fix the *iSpec* analysis to this $\log g$, the metallicity and effective temperature are very similar to the initial results (see Table 2). $\log g$ is not well constrained spectroscopically, and changes have very limited effect on other parameters. Therefore we adopt the $\log g = 3.52$ based parameters.

3.2. Eliminating *K2* Photometric Systematics

Given the high possibility for false positives when dealing with montransits, we have endeavored to reasonably eliminate all causes for false positives. All objects listed as ‘Stars’ with *K2* light curves within 25 arcminutes were checked for similar artifacts. Of the 61 objects, none showed odd behaviour at the same epoch as the montransit. Additionally, the location of EPIC248847494 was not near the edge of the CCD suggesting

Table 2. Properties of the EPIC248847494 system

Parameter	Units	Value
Stellar Parameters:		
2MASS		J10373341+1150338 ^a
α	Right ascension [hh:mm:ss]	10:37:33.42 ^a
δ	Declination [dd:mm:ss]	11:50:33.8 ^a
K_{ep}	[mag]	12.17 ^a
V	[mag]	12.42 ^b
K	[mag]	10.15 ^c
g_{Gaia}	[mag]	12.17 ^d
μ_{α}	Proper motion [mas yr ⁻¹]	-38.74±0.07 ^d
μ_{δ}	Proper motion [mas yr ⁻¹]	1.21±0.06 ^d
$\hat{\pi}$	Parallax [mas]	1.78±0.04 ^d
d	Distance [parsecs]	560±13 [†]
Fe/H	Metallicity [dex]	-0.23±0.04 [†]
T_{eff}	Effective temperature [K]	4898±68 [†]
$\log(g)$	Surface gravity [dex]	3.52 (fixed) [†]
R_*	Radius [R_{sol}]	2.70±0.12 [†]
M_*	Mass [M_{sol}]	0.90±0.09 [†]
ρ_*	Density [g cm ⁻³]	0.064±0.007 [†]
μ_1	Lin. limb-darkening coeff.	0.562 ^{-0.001} _{+0.001}
μ_2	Quad. limb-darkening coeff.	0.149 ^{-0.001} _{+0.001}
Planet Parameters:		
P_{orb}	Period [days]	3650 ⁺¹²⁸⁰ ₋₁₁₃₀ [†]
v'	Orbital velocity [R_* d ⁻¹]	0.61 ^{+0.08} _{-0.05} [†]
T_{C}	Transit centre [BJD]	2457967.17 ^{+0.01} _{-0.01} [†]
T_{D}	Transit duration [hours]	53.6 ^{+5.9} _{-5.3} [†]
R_{P}/R_*	Planet-stellar radii ratio	0.042 ^{+0.002} _{-0.002} [†]
a	Semi-major axis [AU]	4.5 ^{+1.0} _{-1.0} [†]
b	Impact parameter	0.79 ^{+0.04} _{-0.07} [†]
i	Inclination [°]	89.87 ^{+0.02} _{-0.03} [†]
R_{P}	Planet radius [R_{Jup}]	1.11 ^{+0.07} _{-0.07} [†]
$\langle F \rangle$	Incident flux [ergs s ⁻¹ cm ⁻²]	2.6 ^{+1.7} _{-0.9} × 10 ¹⁰ [†]
T_{eq}	Equilibrium temperature [K]	183 ⁺²⁵ ₋₁₈ [†]

^a Huber et al. 2016, ^b APASS: Henden & Munari 2014,

^c 2MASS: Skrutskie et al. 2006,

^d Gaia Collaboration et al. 2018, [†] This Work

no near-edge effects took place. From the Target Pixel file of EPIC248847494, we checked the pixels for changes and failures before (both the star and background flux), during and after the transit – none were found. We checked the centroid shifts of EPIC248847494 in the *K2* release light curves. There are three clear regimes in pointing (times given in BJD-2454833): ~3072-3087 days – *K2* settling into position after changing field; ~3087-3124 days – *K2* approaching optimum stability position; and ~3124-3153 days – *K2* retreating from the optimum stability position. The optimum stability position is the moment when the balance between the remaining reaction wheels of *K2* are most stably balanced against the solar radiation pressure (G. Baretzen, personal communication). The monotransit is away from this optimum stability position and other shifts in pointing. Furthermore, there is no evidence that centroid position for the PSFs or the flux weighted centre have dramatically changed for any reason. Using the extracted light curve from Vanderburg & Johnson (2014), available from MAST², we checked the in-transit points along the measured arc caused by the movement of *K2*. When in-

specting the change in flux due to arclength, no in-transit points were constrained to a single area, but covered the arc uniformly with no evidence for earlier or later points favoring certain arclength positions. No close neighbours are present in the Gaia DR2 data (Gaia Collaboration et al. 2018).

3.3. Planet Parameters

General transit-fitting methods are often unsuitable for modelling monotransits, as intrinsic knowledge of the orbit is necessary (e.g. P and R_*/a), therefore a monotransit-specific fitting code (Namaste, Osborn et al. 2016)³ was used to model the HLSP light curve from Vanderburg & Johnson (2014) of EPIC248847494 and explore the planetary characteristics. It applies the transit models of Mandel & Agol (2002) taking the lateral velocity of the planet (scaled to stellar radius) as a parameter. Other transit parameters required are planet-to-star radius (uniform prior between 0.02 & 0.25), impact parameter (uniform prior between -1.2 & 1.2), transit centre and limb darkening. Quadratic limb darkening coefficients were estimated from T_{eff} , $\log g$ and metallicity for the *Kepler* bandpass (Sing 2010) and fixed using a Gaussian prior.

Emcee (Foreman-Mackey et al. 2016) was used to explore the parameter space of the transit and Gaussian process models. To model the stellar and photon noise present in the light curve we used the *celerite* Gaussian process package (Foreman-Mackey et al. 2017). We fit two GPs, an exponential kernel for long-timescale trends ($\log a = -7.41 \pm 0.72$, $\log c = -10.9 \pm 0.7$), and a matern-3/2 kernel for short-timescale granulation ($\log \sigma = -10.0^{+0.23}_{-1.3}$, $\log \rho = -2.72^{+0.48}_{-0.38}$), alongside a fixed white noise term (90ppm, van Cleve & Caldwell 2009). We also tested the performance of a stellar rotation-like quasi periodic kernel, an artificially high white noise term to account for granulation, and fitting rather than fixing the white noise, all of which gave consistent results.

The best fit is a planet with orbital velocity $v' = 0.61^{+0.08}_{-0.05} R_*$ d⁻¹ which gives an orbital period of 3650⁺¹²⁸⁰₋₁₁₃₀ days, when converted using

$$\left(\frac{P_{\text{circ}}}{d}\right) = 18226 \frac{(\rho_*/\rho_{\odot})}{(v'/d^{-1})^3}. \quad (1)$$

However, the model fitting revealed strong correlations between R_{P}/R_* , b and v' . This suggests a higher velocity, slightly smaller planet on a low-impact parameter transit fits the data almost as well as the larger R_{P}/R_* and b but lower v' . But as R_{P}/R_* only varied by a small amount, it did not significantly vary the planetary radius.

The Namaste fit resulted in a planet-like object with a radius of $1.11 \pm 0.07 R_{\text{Jup}}$, orbiting its host star between 3.5 and 5.5 AU. This would indicate the planet has a temperature of approximately 183^{+25}_{-18} K (with albedo set to 0). For simplicity we assume an eccentricity of 0, although we note that any orbital eccentricity would increase the spread on the velocity and therefore the period. For details, please see Osborn et al. (2016). We hope to constrain this as we gather more long-term RV data.

Knowing the time of transit means we are in a unique position for radial velocity follow-up. For all observations, it is possible to calculate the phase given an orbital period or semi-major axis, and an RV value given a planetary mass. Therefore we construct a grid of semi-major axes, 0.5 to 15AU, and planetary masses, 0.3 to 150 M_{Jup} . From this, we calculate the orbital period and the semi-amplitude for the system, assuming

² <https://archive.stsci.edu/prepds/k2sff/>
³ <https://github.com/hposborn/namaste>

eccentricity is zero. We calculate for each grid point the RVs that would be at the times we have data and determine the RV slope, assuming a linear fit, in m/s/day. In Figure 3, we show the measured RV slope and the 1-, 2- σ errors cover the estimated semi-major axis range from Namaste. The peaks in the grid scale at 0.55, 0.75 and 2 AU are due to RV quadrature for those orbits. In combination with Fig. 2, it is clear that the RV signal would indicate a mass of $13M_{\text{Jup}}$ or less.

We also calculate the minimum RV slope we would expect to see for certain celestial body types in the 4.5 AU orbit from Namaste. For a low-mass star ($>80M_{\text{Jup}}$) and a brown-dwarf ($>13M_{\text{Jup}}$) we would expect to see 1.88 m/s/day and 0.31 m/s/day respectively. Therefore a planet-like object, over ~ 120 days needs to show a change of less than $\sim 36\text{m/s}$ (Fig. 2).

4. Discussion

If EPIC248847494b is indeed planetary in nature and confirmed with RVs, it will be the longest period transiting exoplanet ever discovered. For final confirmation it would require 3 years of radial velocity follow-up. Currently, there is only one confirmed transiting planet in the NASA Exoplanet Archive⁴ (Akeson et al. 2013) with a period longer than 2500 days (our lower limit). With an occurrence rate of $\sim 4.2\%$ (Cumming et al. 2008) for a planet with mass between 0.3 and $15 M_{\text{Jup}}$ in a 3-6 AU orbit and a transit probability of 0.12%, applied to the entire K2 catalogue (312,269 stars) which are observed for a maximum of 80 days, we would expect to detect on the order of one object.

Comparison with planets within the solar system, EPIC248847494b is similar to our gas giants which heavily suggests it will possess moons. As the estimated equilibrium temperature is 183^{+25}_{-18}K , that would indicate the planet is close to the snow line. Therefore, any moons may well be near the habitable zone, based on the stellar effective temperature and luminosity (Kopparapu et al. 2013, 2014) – although it would have been much cooler for most of the star’s main sequence lifetime.

The minimum observing windows for *TESS* are 27.4 days (assuming non-consecutive observing windows). This will apply a hard limit of ~ 28 -day periods for objects to have 2 or more transits. This has recently been investigated by Villanueva et al. (2018) where they have estimated that *TESS* will discover 241 monotransits from the postage stamps and a further 977 from the Full-Frame-Images. With the possibility of over 1000 new, single transit candidates there may be many more EPIC248847494b-type planets to be discovered and characterised.

5. Conclusions

From Campaign 14 of the K2 mission, we detected a monotransit in the light curve of EPIC248847494 and performed follow-up observations. From spectra obtained as radial velocity measurements we determined that EPIC248847494b orbits a $2.70 \pm 0.12 R_{\text{sol}}$ star with a mass of $0.9 \pm 0.09 M_{\text{sol}}$ – a sub-giant star. EPIC248847494b is the first, long-period planet to be vetted using radial velocity, starting from a single monotransit. We estimate the orbital period to be 3650^{+1280}_{-1130} days, a radius of approximately $1.11 \pm 0.07 R_{\text{Jup}}$ with a lower and upper limit on the mass of 1 and $\sim 13 M_{\text{Jup}}$ respectively.

This is an excellent candidate for attempting to detect exomoons which may well be habitable, however this would require

extremely precise photometry (e.g. CHEOPS, Broeg et al. 2013, or PLATO, Rauer et al. 2014) for future transit events.

Additionally, given the shorter observation campaigns from *TESS*, the number of monotransit candidates will increase. We have shown that it is possible, given the parameters that can be measured from the transit, to characterise these candidates and potentially push out to longer and longer orbital periods.

Acknowledgements. We would like to thank the referee for their comments and suggestions – they were extremely valuable for the development of this Letter.

We thank the Swiss National Science Foundation (SNSF) and the Geneva University for their continuous support to our planet search programs. This work has been in particular carried out in the frame of the National Centre for Competence in Research ‘Planets’ supported by the Swiss National Science Foundation (SNSF).

This paper includes data collected by the *Kepler* mission. Funding for the *Kepler* mission is provided by the NASA Science Mission Directorate.

HG acknowledges the assistance from L. Temple on measuring stellar radii.

References

- Akeson, R. L., Chen, X., Ciardi, D., et al. 2013, *PASP*, 125, 989
Blanco-Cuaresma, S., Nordlander, T., Heiter, U., et al. 2016, in 19th Cambridge Workshop on Cool Stars, Stellar Systems, and the Sun (CS19), 22
Blanco-Cuaresma, S., Nordlander, T., Heiter, U., et al. 2017, in Highlights on Spanish Astrophysics IX, ed. S. Arribas, A. Alonso-Herrero, F. Figueras, C. Hernández-Monteagudo, A. Sánchez-Lavega, & S. Pérez-Hoyos, 334–337
Blanco-Cuaresma, S., Soubiran, C., Heiter, U., & Jofré, P. 2014a, *A&A*, 569, A111
Blanco-Cuaresma, S., Soubiran, C., Jofré, P., & Heiter, U. 2014b, *A&A*, 566, A98
Bouchy, F., Moutou, C., Queloz, D., & CoRoT Exoplanet Science Team. 2009, in IAU Symposium, Vol. 253, Transiting Planets, ed. F. Pont, D. Sasselov, & M. J. Holman, 129–139
Broeg, C., Fortier, A., Ehrenreich, D., et al. 2013, in European Physical Journal Web of Conferences, Vol. 47, European Physical Journal Web of Conferences, 03005
Cumming, A., Butler, R. P., Marcy, G. W., et al. 2008, *PASP*, 120, 531
Eggenberger, P., Meynet, G., Maeder, A., et al. 2008, *Ap&SS*, 316, 43
Foreman-Mackey, D., Agol, E., Angus, R., & Ambikasaran, S. 2017, *AJ*, 154, 220
Foreman-Mackey, D., Morton, T. D., Hogg, D. W., Agol, E., & Schölkopf, B. 2016, *AJ*, 152, 206
Fulton, B. J. & Petigura, E. A. 2018, ArXiv e-prints [arXiv:1805.01453]
Gaia Collaboration, Brown, A. G. A., Vallenari, A., et al. 2018, ArXiv e-prints [arXiv:1804.09365]
Giles, H. A. C., Bayliss, D., Espinoza, N., et al. 2018, *MNRAS*, 475, 1809
Gray, R. O. & Corbally, C. J. 1994, *AJ*, 107, 742
Gustafsson, B., Edvardsson, B., Eriksson, K., et al. 2008, *A&A*, 486, 951
Heiter, U., Jofré, P., Gustafsson, B., et al. 2015a, *A&A*, 582, A49
Heiter, U., Lind, K., Asplund, M., et al. 2015b, *Phys. Scr*, 90, 054010
Henden, A. & Munari, U. 2014, Contributions of the Astronomical Observatory Skalnaté Pleso, 43, 518
Houdashelt, M. L., Bell, R. A., & Sweigart, A. V. 2000, *AJ*, 119, 1448
Huber, D., Bryson, S. T., Haas, M. R., et al. 2016, *ApJS*, 224, 2
Jofré, P., Heiter, U., Soubiran, C., et al. 2014, *A&A*, 564, A133
Kopparapu, R. K., Ramirez, R., Kasting, J. F., et al. 2013, *ApJ*, 765, 131
Kopparapu, R. K., Ramirez, R. M., Schottelkotte, J., et al. 2014, *ApJ*, 787, L29
Kovács, G., Zucker, S., & Mazeh, T. 2002, *A&A*, 391, 369
LaCourse, D. M. & Jacobs, T. L. 2018, *Research Notes of the American Astronomical Society*, 2, 28
Mandel, K. & Agol, E. 2002, *ApJ*, 580, L171
Osborn, H. P., Armstrong, D. J., Brown, D. J. A., et al. 2016, *MNRAS*, 457, 2273
Osborn, H. P., Kristiansen, M. H., Armstrong, D. J., Pollacco, D. L., & Deleuil, M. in prep.
Queloz, D., Henry, G. W., Sivan, J. P., et al. 2001, *A&A*, 379, 279
Queloz, D., Mayor, M., Weber, L., et al. 2000, *A&A*, 354, 99
Rauer, H., Catala, C., Aerts, C., et al. 2014, *Experimental Astronomy*, 38, 249
Sing, D. K. 2010, *A&A*, 510, A21
Skrutskie, M. F., Cutri, R. M., Stiening, R., et al. 2006, *AJ*, 131, 1163
van Cleve, J. E. & Caldwell, D. A. 2009, *Kepler Instrument Handbook*, 1st edn.
Vanderburg, A. & Johnson, J. A. 2014, *PASP*, 126, 948
Vanderburg, A., Mann, A. W., Rizzuto, A., et al. 2018, ArXiv e-prints [arXiv:1805.11117]
Vanderburg, A., Montet, B. T., Johnson, J. A., et al. 2015, *ApJ*, 800, 59
Villanueva, Jr., S., Dragomir, D., & Gaudi, B. S. 2018, ArXiv e-prints [arXiv:1805.00956]

⁴ exoplanetarchive.ipac.caltech.edu

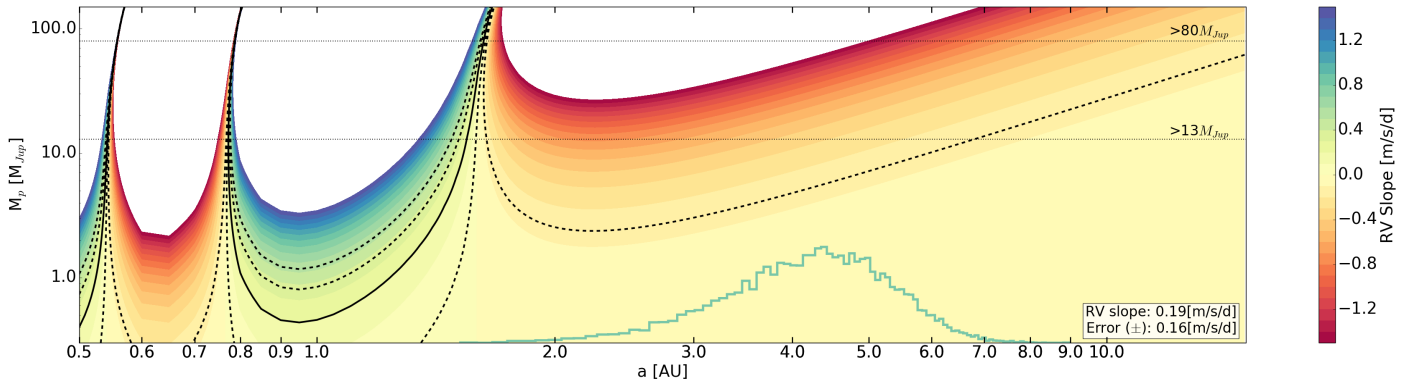


Fig. 3. A grid of semi-major axes and planetary masses and their corresponding RV slopes, using observations from CORALIE. The colour scale ranges -1.5 to 1.5 m/s/day, with all else set to white. The slope, with 1- and 2- σ errors, of the CORALIE RVs (solid and dashed black lines) show regions of likely solutions. Also shown are mass limits for low-mass stars and brown dwarfs (black dashed-lines). The Namaste fit of the light curve (see Sect. 3) produces a distribution of semi-major axes (green histogram). The peaks in the grid scale at 0.55, 0.75 and 2 AU are due to RV quadrature for those orbits.